Cerebral Cortex, February 2019;29: 701–715

doi: 10.1093/cercor/bhx353
Advance Access Publication Date: 24 January 2018
Original Article

ORIGINAL ARTICLE

Fear Extinction Recall Modulates Human Frontomedial Theta and Amygdala Activity

Matthias F. J. Sperl[1,2,3], Christian Panitz[1,2], Isabelle M. Rosso[3], Daniel G. Dillon[3], Poornima Kumar[3], Andrea Hermann[2], Alexis E. Whitton[3], Christiane Hermann[2], Diego A. Pizzagalli[3] and Erik M. Mueller[1,2]

[1]Department of Psychology, Personality Psychology and Assessment, University of Marburg, 35032 Marburg, Germany, [2]Department of Psychology, Clinical Psychology and Psychotherapy, University of Giessen, 35394 Giessen, Germany and [3]Department of Psychiatry, Center for Depression, Anxiety and Stress Research, McLean Hospital, Harvard Medical School, Belmont, MA 02478, USA

Address correspondence to Matthias F.J. Sperl, Department of Psychology, Personality Psychology and Assessment, University of Marburg, Gutenbergstr. 18, 35032 Marburg, Germany. Email: matthias.sperl@staff.uni-marburg.de

Abstract

Human functional magnetic resonance imaging (fMRI) and electroencephalography (EEG) studies, as well as animal studies, indicate that the amygdala and frontomedial brain regions are critically involved in conditioned fear and that frontomedial oscillations in the theta range (4–8 Hz) may support communication between these brain regions. However, few studies have used a multimodal approach to probe interactions among these key regions in humans. Here, our goal was to bridge the gap between prior human fMRI, EEG, and animal findings. Using simultaneous EEG–fMRI recordings 24 h after fear conditioning and extinction, conditioned stimuli presented (CS+E, CS−E) and not presented during extinction (CS+N, CS−N) were compared to identify effects specific to extinction versus fear recall. Differential (CS+ vs. CS−) electrodermal, frontomedial theta (EEG) and amygdala responses (fMRI) were reduced for extinguished versus nonextinguished stimuli. Importantly, effects on theta power covaried with effects on amygdala activation. Fear and extinction recall as indicated by theta explained 60% of the variance for the analogous effect in the right amygdala. Our findings show for the first time the interplay of amygdala and frontomedial theta activity during fear and extinction recall in humans and provide insight into neural circuits consistently linked with top-down amygdala modulation in rodents.

Key words: fear conditioning, fear extinction, frontal-midline theta, simultaneous EEG–fMRI, threat processing

Introduction

Elucidating brain mechanisms of conditioned and extinguished fear recall is crucial for understanding pathological processes underlying anxiety disorders and for developing interventions to enhance extinction learning (Bowers and Ressler 2015). Anatomically, human fear expression is associated with increased activation in the amygdala (Kim and Jung 2006; LeDoux 2014; but see Fullana et al. 2016), insula (Kim and Jung 2006; Fullana et al. 2016), and anterior midcingulate cortex (AMC) (Milad et al. 2007a; Fullana et al. 2016), whereas recall of extinguished fear is commonly linked to increased ventromedial prefrontal cortex (vmPFC) activation (Kalisch et al. 2006; Milad et al. 2007b; Milad and Quirk 2012; Hermann et al. 2016) and decreased amygdala activation (Phelps et al. 2004; Hermann et al. 2016). The amygdala is thought to mediate fear learning and fear expression (LeDoux 2014; Hermans et al. 2017). It serves as a hub for fear-related processes (Milad and Quirk 2012; Kim and Cho 2017), receiving input from prefrontal

regions involved in fear expression and regulation (Hartley and Phelps 2009; Pitman et al. 2012). Importantly, the AMC has excitatory projections to the amygdala during fear recall (Gilmartin et al. 2014), which regulate physiological fear responses (Hartley and Phelps 2009; Panitz et al. 2015). Conversely, inhibition of the fear response during extinction recall is mediated by projections from the vmPFC to intercalated cells in the amygdala (Quirk and Mueller 2008; Pitman et al. 2012), presumably modulated by hippocampal activation (Milad and Quirk 2012; Merz et al. 2014).

Studies investigating fear extinction in rodents have identified homologous prefrontal brain regions. Specifically, stimulation of the rodent prelimbic cortex (PL), which is considered the homolog of the human AMC (Milad and Quirk 2012), increases fear expression (Vidal-Gonzalez et al. 2006). Similarly, inactivation of the infralimbic cortex (IL), a homologous region to the human vmPFC (Milad and Quirk 2012), impairs fear extinction (Sierra-Mercado et al. 2011; Lingawi et al. 2016). Although there is evidence from rodent single-cell recording studies that the amygdala is crucial for triggering fear responses (Repa et al. 2001), the duration of CS evoked amygdala responses is very short (Quirk et al. 1995; Goosens and Maren 2004). Conversely, PL theta (i.e., 4–8 Hz) oscillations are assumed to be relevant for initiating more sustained fear processing at neural and behavioral levels (Burgos-Robles et al. 2009; Pitman et al. 2012). Specifically, rodent PL neurons show a sustained response to previously fear-conditioned and nonextinguished stimuli by a change in their firing rate from 2 Hz to the theta range (i.e., ~4–8 Hz; Burgos-Robles et al. 2009), and theta synchrony may be crucial for amygdala-AMC connectivity (Gilmartin et al. 2014). Importantly, the PL may receive information about CS salience from the amygdala (Gilmartin et al. 2014; Senn et al. 2014), while projections from the PL to the amygdala may provide information regarding the predictive value of the CS (Courtin et al. 2014; Gilmartin et al. 2014).

Converging with these animal studies, a recent human 64-channel EEG study (Mueller et al. 2014b) showed that healthy subjects displayed enhanced theta oscillations (4–8 Hz) at frontomedial EEG electrodes during the presentation of previously fear-conditioned and nonextinguished stimuli, which were source-localized to the AMC (Mueller et al. 2014b). Consistent with a key role in fear expression and extinction, frontal-midline theta has also been consistently linked to state and trait anxiety in humans (Mitchell et al. 2008; Mueller et al. 2014a; Cavanagh and Shackman 2015) and is modulated by anxiolytic drugs (Mitchell et al. 2008). Importantly, brain oscillations not only relate to threat processing, but also can be conceptualized as reflecting neural mechanisms of cognitive processes (Lopes da Silva 2013). Synchronous oscillations are crucially involved in linking brain areas within functional networks (Klimesch 1996; Bastiaansen, Mazaheri, Jesen 2012). Theta oscillations are of particular relevance for modulating and gating information transfer among specific neuronal populations (Mizuseki et al. 2009; Lopes da Silva 2013), including communication between prefrontal brain areas and the amygdala (Gilmartin et al. 2014). Notably, in mice, altered theta synchronization in the amygdala–prefrontal cortex network has been associated with fear extinction recall (Narayanan et al. 2011).

While animal studies have significantly helped to develop plausible neural models of fear learning, the limited temporal and spatial resolution of functional magnetic resonance imaging (fMRI) and electroencephalography (EEG), respectively, have limited the generalization of insights from animal single-cell recording studies to humans. Taken together, electrophysiological findings suggest that frontomedial theta oscillations are essential for anxiety and fear-related processes not only in animals (Likhtik and Gordon 2014), but also in humans (Mueller et al. 2014a, 2014b; Cavanagh and Shackman 2015). Conversely, fMRI has been widely used to study fear conditioning and extinction in humans (Milad and Quirk 2012), and has consistently highlighted the amygdala as a hub region for fear processing (Phelps and LeDoux 2005; Janak and Tye 2015). However, because these findings emerge from different imaging modalities, it remains unclear how they can be integrated and how amygdala processes and theta oscillations are functionally connected in humans. In particular, the integration of models for amygdala activation with frontomedial theta oscillations cannot be assessed with fMRI or EEG in isolation. The aim of the present study is to bridge the gap between prior animal studies, human EEG, and human fMRI findings by recording EEG and fMRI simultaneously.

To address this question, we used an established 2-day fear conditioning and extinction paradigm (Fig. 1) (Mueller et al. 2014b). During fear acquisition, 2 conditioned stimuli (CS+) were repeatedly paired with an aversive unconditioned stimulus (US), while 2 additional conditioned stimuli (CS–) were never followed by a US. In the subsequent extinction phase, 1 of the 2 CS+ ("CS+E") and one CS– ("CS–E") were presented without the US, and thus responses to those stimuli were extinguished. The other CS+ ("CS+N") and CS– ("CS–N") were not presented, thus leaving learned responses to those stimuli fully intact. During a recall test approximately 24 h later, EEG and fMRI were recorded simultaneously. To identify effects specific to extinction versus fear recall, differential hemodynamic and electrophysiological responses to extinguished (CS+E vs. CS–E) and nonextinguished conditioned stimuli (CS+N vs. CS–N) were compared. Our data revealed the expected interplay of amygdala activation and frontomedial theta oscillations, thus extending key insights from animal research into the human realm. Theta activity appears to play a dominant role in communication between the amygdala and the prefrontal cortex during human fear and extinction recall (FER).

Materials and Methods

Subjects

A total of 21 healthy students at Justus Liebig University Giessen were recruited for this study. Three subjects were excluded from the analysis due to complete absence of explicit CS–US contingency awareness after acquisition (defined as higher awareness ratings for CS– than CS+), resulting in a final sample of 18 right-handed and nonsmoking subjects (mean age = 22.72 years, standard deviation [SD] = 3.34 years, range: 19–29 years; 50% females; see also Supplementary Material H). All subjects participated either for partial fulfillment of course credit or were reimbursed with 10 €/h, and gave written informed consent to participate. As there is evidence for an influence of menstrual cycle phase on fear conditioning and extinction (Hwang et al. 2015), only female participants who took oral contraceptives on a regular basis were recruited. Moreover, they were tested during their pill intake phase in order to reduce variance related to fluctuations of gonadal hormones. Exclusion criteria were a history of mental (assessed by the short version of the Diagnostic Interview for Mental Disorders, Mini-DIPS; Margraf 1994), neurological, or cardiovascular disorders,

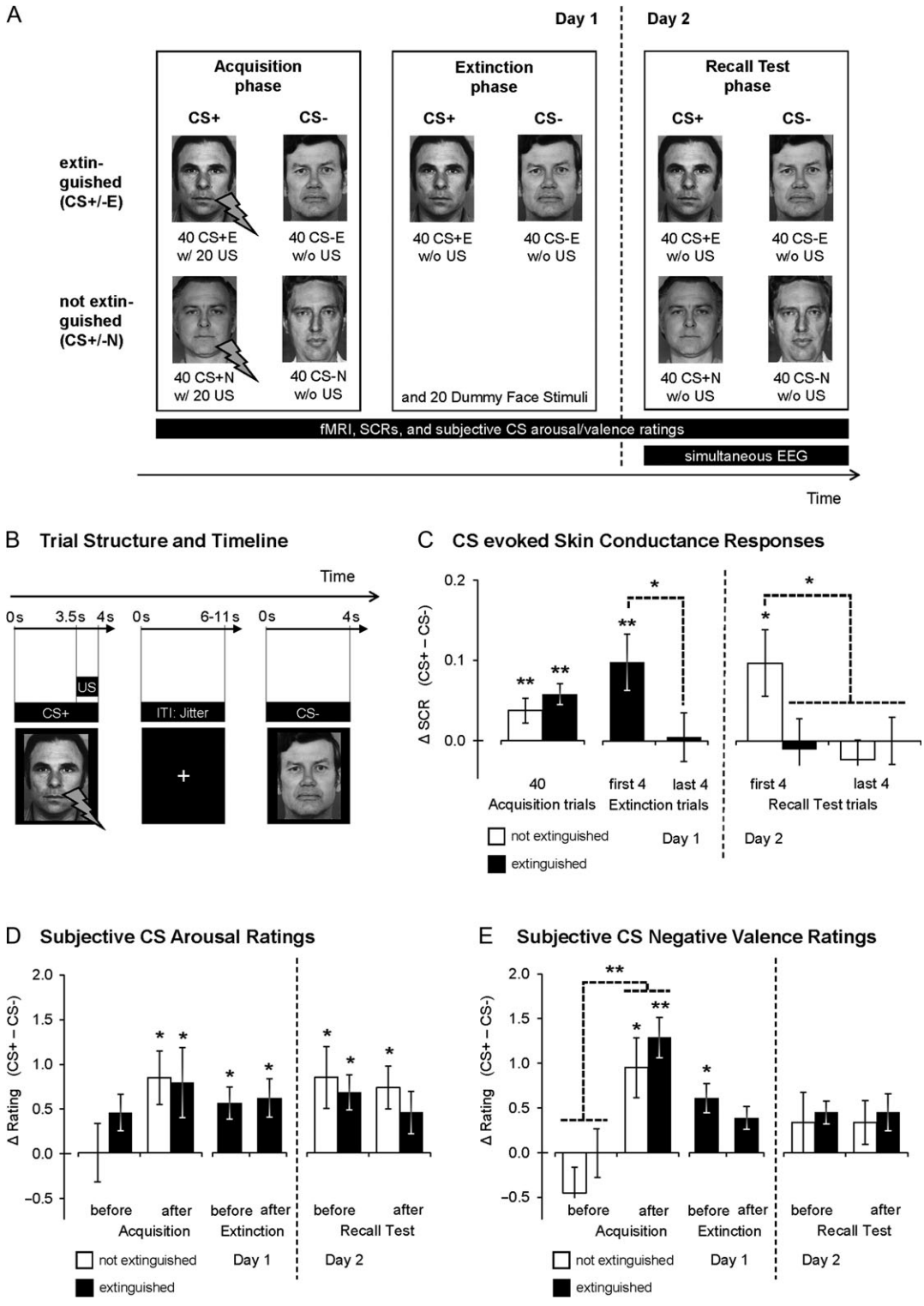

Figure 1. Schematic depiction of the experimental paradigm used in the present study. (*A*) Number and stimuli types presented during the 3 experimental phases. The central hypotheses of the current study focused on the Day 2 recall test, during which EEG and fMRI were recorded simultaneously. CS+E/CS–E, CSs presented during extinction phase; CS+N/CS–N, CSs not presented during extinction phase. CS+ were reinforced with an aversive US ("w/", contingency of 50%) during acquisition phase, while CS– were never paired with a US ("w/o"). (*B*) Trial structure and timeline for a single CS trial. All CSs were shown for 4 s. During the acquisition phase, a 500-ms electric shock US coterminated with 50% of all CS+ trials, starting 3.5 s after CS onset. (*C*) Normalized CS evoked differential (CS+ – CS–) SCRs, (*D*) subjective CS arousal ratings, and (*E*) subjective CS negative valence ratings ($M \pm$ within-subject standard error of the mean (SEM), O'Brien and Cousineau 2014) for extinguished and nonextinguished stimuli during all experimental stages. $^{*}P \leq 0.05$, $^{**}P \leq 0.01$ (one-sided, CS+ > CS–).

or a report of MRI exclusion criteria. Furthermore, subjects were excluded if they reported using illegal drugs or prescription drugs that affect the central nervous system. All subjects had normal or corrected-to-normal vision and were asked to refrain from alcoholic or caffeinated drinks, heavy meals, and strenuous exercise prior to the experiment. The study protocol was approved by the local ethics committee of the Faculty of Psychology and Sports Science at Justus Liebig University Giessen.

Experimental Paradigm

A 2-day fear conditioning and extinction paradigm (Mueller et al. 2014b) was adapted for simultaneous EEG–fMRI recordings (Fig. 1). During acquisition (Day 1), 2 CS+ (CS+E, CS+N) and 2 CS– (CS–E, CS–N) were presented 40 times each in random order, while both CS+ coterminated with an aversive US in 50% of the trials. All CSs were shown 4 times prior to acquisition without any US pairings to familiarize participants with the stimuli. Approximately 20 min after acquisition, subjects completed an extinction phase, during which only 1 of the 2 CS+ (i.e., extinguished CS+, CS+E) and 1 of the 2 CS– (i.e., CS–E) were presented 40 times each in random order. The other 2 CSs (i.e., nonextinguished CSs, CS+N and CS–N) and the US were not presented during extinction. In order to maintain some variability of stimuli shown during extinction, a novel face ("Dummy Stimulus") was presented 20 times. Approximately 24 h later, all extinguished and nonextinguished stimuli were shown 40 times each in random order without any US presentation. Recall of extinguished fear can be distinguished from recall of conditioned fear by comparing extinguished (CS+/–E) and nonextinguished (CS+/–N) stimuli.

Conditioned and Unconditioned Stimuli

Four different black-and-white pictures of male faces with a neutral expression (Ekman and Friesen 1976) constituted the CSs. The assignment of face stimuli to CS+E, CS+N, CS–E, and CS–N was permutated in a counterbalanced fashion. We confirmed that after the exclusion of 3 contingency unaware subjects (see Subjects) reasonable counterbalancing was still achieved (Supplementary Material A). Specifically, there was no significant association between any CS type (e.g., CS+E) and assignment of particular face stimuli, $x^2(3) = 1.11$, exact $P = 0.859$. All faces were presented for 4 s with a jittered intertrial interval (defined as CS offset to CS onset) of 6–11 s. During the intertrial interval, a white fixation cross was shown on a black background. Visual stimuli were presented on an MR-compatible 32-in visual stimulation system (NordicNeuroLab, Bergen, Norway), while subjects were able to look at the screen by a mirror that was mounted to the head coil (visual angle = 28°). An eye camera (ViewPoint PC-60, Arrington Research, Scottsdale, AZ, USA) was also placed at the head coil in order to check whether subjects had their eyes open and watched the stimuli.

The US consisted of a 500-ms multipulse (1-ms pulses, 50 Hz) electrical stimulation which was delivered from a transcutaneous current stimulator (E13-22, Coulbourn, Allentown, PA, USA) using 2 custom-made steel disk electrodes attached to the middle of the left lower leg (surface size: 1.8 mm^2). During a work-up procedure, the intensity of the shocks ($M = 1.76$ mA, $SD = 0.92$ mA) was set individually to a level which was subjectively perceived as "difficult to bear, but acceptable." Additionally, participants had to rate negative valence of the US higher than 6 on an 11-point Likert scale (0 = not unpleasant at all, 10 = extremely unpleasant) at least 3 times in a row. As the paradigm consists of many trials, which are necessary to ensure an adequate signal-to-noise ratio for EEG analyses, habituation to the US is a potential issue, when conventional shock intensities are used (Sperl et al. 2016). We therefore used a work-up procedure that leads to a slightly higher shock intensity compared with previous peripheral physiological or fMRI studies on fear conditioning (e.g., compared with Hermann et al. 2016). Shock electrodes were attached during all experimental phases.

Subjective CS Ratings

Prior to and after each experimental stage, subjects were asked to rate perceived arousal (1 = not arousing; 5 = very arousing) and valence (1 = very pleasant; 5 = very unpleasant) of each CS on a 5-point Likert scale. For the extinction phase, ratings were restricted to CS+E and CS–E. During acquisition and Day 2 recall phases, additional ratings were requested in the middle of the experimental stages. In addition, subjective awareness of the CS–US contingency was assessed on a 4-point Likert scale (0 = CS was never followed by US; 3 = CS was always followed by US) after acquisition.

In order to evaluate conditioning and extinction on subjective ratings, three-way repeated-measures analyses of variance (ANOVAs) with "Contingency" (CS+ vs. CS–), "Extinction Status" (E vs. N) and "Time" (prior to vs. after acquisition, extinction, or recall phase, respectively) were carried out for each experimental phase. The factor Time was included as we expected an increase of differential ratings (CS+E, CS+N vs. CS–E, CS–N) during acquisition followed by a decrease during extinction. Importantly, FER on Day 2 can be assessed by comparing differential ratings for nonextinguished versus extinguished CSs prior to the recall test.

SCR Data Acquisition and Analyses

Skin conductance was recorded using an additional channel (GSR-MR sensor) of the BrainAmp-MR EEG system (Brain Products, Munich, Germany). Two Ag/AgCl electrodes of a 6-mm diameter filled with isotonic (0.5% NaCl) electrolyte medium were placed on the hypothenar eminence of the left hand. Data were low-pass filtered online (Day 1: 250 Hz, sampling rate 1 kHz; Day 2 during simultaneous EEG: 1 kHz, sampling rate 5 kHz), and afterwards a 0.5 Hz low-pass filter was applied offline. After manually checking for artifacts, for each CS trial a skin conductance response (SCR) score was calculated (Milad et al. 2007b) by subtracting the peak response within 5 s after CS onset from a 1 s pre-CS baseline. This approach, that is, calculating the cumulative maximum conductance change after CS onset for quantification of SCRs (rather than distinguishing between early and late intervals) has been recommended by Pineles, Orr, and Orr (2009) for CS–US intervals as in the present study and is consistent with many human fear conditioning studies (Lonsdorf et al. 2017). Following established procedures (Lykken and Venables 1971), individual SCRs were normalized by dividing the raw SCR value of each CS by an individual's maximum SCR value across all CS (separately for experimental phases). Afterwards, SCR scores were averaged across trials for each CS type. During fear acquisition, successful conditioning is reflected by higher SCRs for unpaired CS+ (CS+E, CS+N) compared with CS– (CS–E, CS–N), which was tested using a two-way repeated-measures ANOVA with the factors Contingency (CS+ vs. CS–) and Later Extinction Status (E vs. N). We expected a decline of this conditioned response (CS+E vs. CS–E) from early (first 4 trials) to late (last 4 trials) extinction learning

(Milad et al. 2013, Contingency × Time ANOVA). Successful FER on Day 2 can be demonstrated by higher SCRs for CS+N compared with CS−N, but not for CS+E compared with CS−E. Due to a quick habituation of fear-conditioned SCRs (Lonsdorf et al. 2017), we expected this effect during the first 4 recall trials (as in prior studies; Milad et al. 2007b; Hermann et al. 2016), but not toward the end of the recall phase. Similar to the analyses on affective ratings, we computed a Contingency × Extinction Status × Time (first vs. last 4 recall trials) ANOVA. To explicitly test for a differential habituation of fear-conditioned and extinguished SCRs (i.e., fear recall leading to an elevated SCR response to the CS+N in the first 4 trials as compared with all other stimuli and as compared with the last 4 trials), we specified the transformation coefficients matrix for the following customized hypothesis test: [CS+N first 4 trials (contrast coefficient = +7)] vs. [CS+E first (−1), CS+E last (−1), CS+N last (−1), CS−E first (−1), CS−E last (−1), CS−N first (−1), CS−N last (−1) 4 trials].

fMRI Data Acquisition and Analyses

Functional and structural data were acquired using a Siemens MRI Scanner MAGNETOM Prisma (3.0 T, Siemens Healthineers, Erlangen, Germany) with an XR 80/200 gradient coil and a Head/Neck 64-channel coil. For functional images, T2*-weighted gradient echo-planar imaging sequences (Siemens WIP883A, based on ep2d_bold) with 40 slices covering the whole brain were applied (slice thickness: 3 mm, interslice gap: 0.75 mm; descending slice procedure; TR = 2500 ms; TE = 30 ms; flip angle = 75°; field of view: 192 × 192 mm^2; voxel size: 3 × 3 × 3 mm^3; GRAPPA: acceleration factor 2). For the acquisition and recall phases, 841 volumes were collected, while 507 volumes were acquired during extinction. In order to minimize susceptibility artifacts in prefrontal brain areas, orientation of axial slices was set with autoalign (Head-Brain) and an additional angle of −30° transversal to coronal. For the normalization procedure, 176 T1-weighted structural images (MPRAGE, slice thickness: 0.94 mm; TR = 1580 ms; TE = 2.3 ms; field of view: 240 × 240 mm^2; voxel size: 0.94 × 0.94 × 0.94 mm^3; GRAPPA: acceleration factor 3) were acquired in sagittal orientation. Moreover, a gradient echo field map was collected for unwarping of B_0 distortions.

All analyses of fMRI data were performed in SPM12 (Wellcome Department of Cognitive Neurology, London, UK), implemented in MATLAB 8.6 (MathWorks, Natick, MA, USA). Each experimental session was analyzed separately. Preprocessing of fMRI data included unwarping and realignment, slice time correction, co-registration to the structural image of each subject, segmentation into different tissue types, normalization ("unified model" implemented in SPM12 which includes linear and nonlinear transformations) to the standard space of the Montreal Neurological Institute (MNI) brain with a voxel size of 2 × 2 × 2 mm^3, and spatial smoothing with an isotropic 3D Gaussian kernel (FWHM: 4 mm). Furthermore, outliers in the temporal scan-to-scan difference series were identified using Artifact Detection Toolbox (ART; McGovern Institute for Brain Research, Cambridge, MA, USA). Extreme volumes with regard to global signal intensity (>3 SD of average signal intensity across scans) and translational movement (>0.5 mm) were modeled as outliers in the first-level analysis. In addition, head motion parameters (3 translation parameters, 3 rotation parameters, 1 composite motion parameter which contains the maximum scan-to-scan movement) were included as first-level regressors.

For the acquisition phase, the first-level general linear model (GLM) contained the following 3 task-related regressors: CS+ (CS+E and CS+N combined), CS− (CS−E and CS−N combined), and US. To confirm that neural responses did not differ between to-be extinguished and to-be nonextinguished stimuli during acquisition, we constructed an additional first-level GLM which contained separate regressors for to-be extinguished and to-be nonextinguished CS+/CS−. As the analysis on CS+ was restricted to unreinforced stimuli (not paired with US), this regressor was split into 2 regressors (paired CS+ and unpaired CS+). For the extinction phase, CS+E, CS−E, and Dummy Stimulus were included as regressors. For Day 2 recall, the first-level model consisted of CS+E, CS+N, CS−E, and CS−N. The ratings of CSs in the middle of the acquisition and recall phases were modeled as additional regressors, while volumes collected during the ratings at the beginning and end of each phase were discarded. All previously described regressors were modeled by a block function with the length of the events which was convolved with the hemodynamic response function in the GLM of the first-level analysis. In order to remove slow signal drifts, a high-pass filter with a time constant of 128 s was applied. For the acquisition and extinction stages, contrasts for conditioned responses (CS+ vs. CS−) were computed for each subject and tested in one-sample *t*-tests during the second-level random effects group analysis (i.e., *t*-tests for previously specified first-level contrasts > 0). For evaluating FER on Day 2, the contrast [(CS+N − CS−N) versus (CS+E − CS−E)] was calculated to compare differential fear responses for nonextinguished (CS+N − CS−N) and extinguished stimuli (CS+E − CS−E).

For all contrasts, both region of interest (ROI) analyses and exploratory whole brain analyses were performed. ROIs contained main structures that have been consistently implicated in fear and extinction (Milad and Quirk 2012; Hermann et al. 2016): amygdala, AMC, hippocampus, insula, and vmPFC. The masks for AMC and vmPFC were created in the MARINA software package (Walter et al. 2003) according to the parcellation of Tzourio-Mazoyer et al. (2002), and were identical to the ones used in previous studies (Hermann et al. 2009; Pejic et al. 2013; Hermann, Keck, Stark 2014). The AMC mask consists of the bilateral cingulate and paracingulate gyri and ranges from *y* = 32 to *y* = −18 (MNI coordinates) with regard to the AC-PC line (Supplementary Material B, see Supplementary Fig. S2A). This mask includes the 2 peak coordinates reported in a recently published meta-analysis on fear conditioning (Fullana et al. 2016). The vmPFC mask consists of the bilateral medial orbital area of the frontal cortex and the gyrus rectus (Supplementary Material B, see Supplementary Fig. S2B), including the 2 peak voxels identified by a meta-analysis on fear extinction (Diekhof et al. 2011). All other masks were maximum probability masks taken from the Harvard-Oxford Cortical and Subcortical Structural Atlases (Harvard Center for Morphometric Analyses, Charlestown, MA, USA) with the probability threshold at 0.50. For exploratory whole brain analyses, a significance threshold of $P \leq 0.05$ on voxel level (family-wise error [FWE] correction for multiple comparisons) with a minimal cluster size (*k*) of 10 voxels was used. All ROI analyses were computed using the small volume correction option of SPM12, while the significance threshold was set to $P \leq 0.05$ on voxel level (FWE-correction). With the exception of AMC and vmPFC masks, all ROIs were tested separately for the left and right hemisphere (Merz et al. 2014).

Analyses of BOLD responses were collapsed across all trials of each experimental phase. Previous fMRI studies of human fear conditioning accounted for a rapid decrease of CS evoked BOLD modulations over time, which is of particular relevance for recall tests without continuing US presentations (Büchel

et al. 1998; Armony and Dolan 2001; Milad et al. 2007b, 2013; Hermann et al. 2016). To increase comparability with other fMRI studies, we accounted for a decrease of BOLD activation over time for the analysis on Day 2 recall, that is, the experimental phase of critical relevance for our hypotheses. Specifically, there is evidence that habituation of amygdala activation can be best characterized by an exponentially decaying function (Büchel et al. 1998; Büchel et al. 1999; Armony and Dolan 2001). Furthermore, habituation of CS evoked SCRs during fear recall (Sperl et al. 2016; Lonsdorf et al. 2017) is correlated with amygdala habituation (Büchel et al. 1998; Phelps et al. 2004; Knight et al. 2005). Consequently, when considering the exponentially decaying function $y = a \cdot e^{-bx}$ we estimated parameters a and b for showing the best fit to the trial-wise habituation of group and CS condition averaged SCRs (Curve Fitting Toolbox 3.5.2, implemented in MATLAB 8.6; MathWorks, Natick, MA, USA). Due to considerable variance of mean SCRs during the second half of the recall test, curve fitting was limited to SCRs of the first half, resulting in $a = 0.28$ and $b = 0.35$ (goodness of fit: $R^2 = 0.62$). Afterwards, for each CS type, an additional regressor was added in the first-level model as parametric modulator which was multiplied with the previously fit function for all recall trials.

To enhance comparability with studies of Milad and colleagues (Milad et al. 2007b, 2009; Milad et al. 2013; Hermann et al. 2016) and to further evaluate the validity of our findings, we performed an additional analysis for Day 2 recall which was restricted to the first 4 trials of each CS type. Therefore, instead of applying an exponential modulation, CS regressors of the first-level GLM were split into 10 regressors of 4 trials each. Our main findings on amygdala activation could be confirmed with both strategies. Corresponding to previous studies on fear/extinction recall (Milad et al. 2009), no significant brain correlates could be found if we did not use any of these strategies to account for habituation of BOLD responses over time.

Finally, for illustration purposes and to perform post hoc control analyses, we extracted contrast estimates using MarsBaR Toolbox (Brett et al. 2002). Contrast estimates represent mean values for an activated cluster of voxels with $P \leq 0.005$ (uncorrected) surrounding FWE-corrected activation peaks.

EEG Data Acquisition and Analyses

During Day 2 recall, EEG was recorded simultaneously inside the MRI scanner (BrainAmp-MR, Brain Products, Munich, Germany), using 31 sintered Ag/AgCl ring electrodes attached to the EEG cap (BrainCap-MR 32 Channels, Easycap, Herrsching, Germany). During recording, an additional electrode at FCz served as reference and an electrode at AFz was used as ground electrode. Electrode impedance was kept below 5 kΩ prior to recording. One remaining channel of the EEG system was used to record the electrocardiogram (ECG), which was used for subtracting heartbeat artifacts during the EEG analysis. In order to prevent pump-induced subject movements, the helium-pump of the MR system was switched off during simultaneous EEG–fMRI. Furthermore, the clock of the EEG system and of the MRI gradient system were synchronized (SyncBox, Brain Products, Munich, Germany) to enhance the quality of MRI artifact subtraction procedures for EEG data and to reduce timing-related errors. The sampling rate was 5 kHz, which is required for artifact reduction procedures. EEG and ECG were band-pass filtered (0.016–250 Hz) online.

EEG preprocessing was performed in BrainVision Analyzer 2.0.2 (Brain Products, Munich, Germany). Corrections for MR gradient and cardioballistic artifacts were applied to EEG data according to adapted versions (Sammer et al. 2005) of the algorithms described by Allen and colleagues (Allen et al. 1998, 2000). A scanner artifact template was created, containing only little EEG contribution, by averaging all EEG segments which interfered with fMRI scanning. The volume-marker of the MR scanner was used to detect scanner artifacts and the segment length was one TR. This correction template was subtracted from each EEG segment. In order to remove residual frequencies without physiological origin, data were low-pass filtered (cutoff at 40 Hz). Cardioballistic artifacts were reduced in a second step. Similar to the reduction of gradient artifacts, an average pulse curve (derived from the 12–20 Hz notch filtered ECG data) was subtracted from the EEG. The correction method accounted for the time delay between the heartbeat and the following artifact in the EEG, which was calculated based on the entire dataset. For the calculation of the correction template, 21 pulse intervals were averaged.

Afterwards, the EEG was manually screened for artifacts, high-pass filtered (0.5 Hz), eye-blink/movement corrected using Independent Component Analysis (ICA), re-referenced to the average reference and segmented into epochs from 0 to 2 s post-CS (Mueller et al. 2014b). To ensure theta findings were not unduly affected by potential artifacts introduced by the ICA-based eye-movement correction, we performed an additional control analysis without ICA eye blink/movement correction. This control analysis included only epochs that were considered to be artifact-free, and the main results were confirmed (Supplementary Material C, see Supplementary Fig. S3A). Information on the residual number of trials per condition after artifact rejection is provided for both analyses (with and without ICA correction) in Supplementary Material D (see Supplementary Fig. S3B). To assess scalp power within the theta band (4–8 Hz; Mueller et al. 2014b) at frontal-midline channel Fz (Mueller et al. 2014b), Fast Fourier Transform (FFT) was applied (Hamming Window length: 10%). The estimated single-trial power was averaged across all trials for each CS and ln-transformed (Mueller et al. 2014a). For illustration purposes, the spectral line values were scaled as if they were calculated with a spectral line spacing of 1 Hz (i.e., μV^2/Hz). FER recall on Day 2 was assessed by comparing differential conditioned responses (CS+ vs. CS−) for nonextinguished and extinguished stimuli. Therefore, we computed a two-way repeated-measures ANOVA, including Contingency (CS+ vs. CS−) and Extinction Status (E vs. N) as repeated-measure factors.

Integration of fMRI and EEG Analyses

The primary goal of the present study was to bridge the gap between electrophysiological and hemodynamic correlates of FER, and to further integrate (1) theta oscillations on the one hand and (2) fear and extinction networks identified by fMRI on the other hand. To address this issue, we computed for each subject a score for theta power at frontal-midline channel Fz which reflects the degree of differential modulation to nonextinguished versus extinguished conditioned stimuli. As in our previous study (Mueller et al. 2014b), this FER score is computed as FER = (CS+N − CS−N) − (CS+E − CS−E). High FER scores indicate that differential fear responses with regard to theta power are higher for nonextinguished (CS+N − CS−N) compared with extinguished (CS+E − CS−E) stimuli during Day 2 recall. Thus, high FER scores are an indicator for successful recall of both conditioned fear (i.e., relatively larger fear response for nonextinguished stimuli) and extinguished fear (i.e., reduced fear

response for extinguished stimuli). In order to integrate fMRI and EEG findings for Day 2 recall, we computed simple regression analysis with theta FER scores (for each subject) as a covariate in the second-level group analysis. Regression analysis was performed with the BOLD response for the FER contrast representing recall of conditioned and extinguished fear as criterion, that is, [(CS+N – CS–N) vs. (CS+E – CS–E)]. For additional analyses on a trial-by-trial coupling of EEG theta oscillations and fMRI activation see Supplementary Material I.

Statistical Analyses

Except for fMRI data, which were analyzed in SPM12 (Wellcome Department of Cognitive Neurology, London, UK) as described above, statistical tests on other physiological data (EEG theta, SCRs) and subjective data (ratings of arousal, valence, and contingency awareness) were performed using SPSS 22 for Windows (IBM, Armonk, NY, USA). For statistical significance, $P \leq 0.05$ (two-sided) was required. For ANOVA analyses, significant interactions involving the factor Contingency (CS+ vs. CS–) were further analyzed using follow-up *t*-tests. As we had a priori hypotheses regarding the direction of the conditioned response (i.e., higher ratings of arousal and negative valence, larger SCRs, and higher theta power for CS+ relative to CS–), one-tailed paired-samples *t*-tests were used to compare CS+E/CS+N and CS–E/CS–N.

Results

Day 1 Fear Conditioning

CS evoked SCRs and affective CS ratings during the acquisition phase confirmed successful fear acquisition on Day 1. Figure 1C shows that during acquisition the 2 CS+ were associated with significantly higher SCR amplitudes than the 2 CS– (main effect of Contingency, $F(1,17) = 18.75$, $P < 0.001$). The absence of a significant Contingency × Later Extinction Status interaction ($F(1,17) = 1.13$, $P = 0.302$) confirmed that SCRs did not differ between to-be extinguished (CS+E = 0.10 ± 0.10; CS–E = 0.04 ± 0.05; $t(17) = 3.12$, $P = 0.003$, one-sided) and to-be nonextinguished (CS+N = 0.08 ± 0.05; CS–N = 0.04 ± 0.05; $t(17) = 4.13$, $P < 0.001$, one-sided) stimuli prior to the extinction phase.

Complementing these findings, relative to the CS–, the 2 CS+ were evaluated as significantly more unpleasant, more arousing, and more likely to be followed by a US after the acquisition phase (Fig. 1D,E). For negative valence ratings of the CS, the Contingency × Later Extinction Status × Time ANOVA revealed a significant interaction of Contingency and Time, $F(1,17) = 12.51$, $P = 0.003$. Both CS+ were rated as significantly more unpleasant after (main effect of Contingency, $F(1,17) = 10.56$, $P = 0.005$), but not prior to, the acquisition phase (main effect of Contingency, $F(1,17) = 2.52$, $P = 0.131$). There was no significant interaction involving the factor Later Extinction Status (Ps ≥ 0.115), indicating similar levels of conditioning for to-be extinguished (5-point scale after acquisition: CS+E = 4.11 ± 0.83; CS–E = 2.83 ± 0.99; $t(17) = 3.75$, $P = 0.001$, one-sided) and to-be nonextinguished (CS+N = 3.83 ± 1.20; CS–N = 2.89 ± 1.18; $t(17) = 2.15$, $P = 0.023$, one-sided) stimuli. For arousal ratings of the CS, a significant main effect of Contingency showed higher ratings for CS+ versus CS–, $F(1,17) = 5.07$, $P = 0.038$. Despite the absence of a Contingency × Time interaction, $F(1,17) = 1.36$, $P = 0.260$, results of separate two-way ANOVAs for each time point confirmed a significant conditioned response after (main effect of Contingency: $F(1,17) = 4.96$, $P = 0.040$), but not prior to the acquisition phase (main effect of Contingency: $F(1,17) = 0.70$, $P = 0.415$). CS+E (5-point scale: 3.28 ± 1.07; $t(17) = 1.87$, $P = 0.040$, one-sided) and CS+N (3.11 ± 1.08; $t(17) = 2.19$, $P = 0.022$, one-sided) were rated as significantly more arousing than CS–E (2.50 ± 1.10) and CS–N (2.28 ± 1.23) after fear acquisition. For CS–US contingency awareness ratings after fear acquisition, the Contingency × Later Extinction Status ANOVA revealed a significant main effect of Contingency, $F(1,17) = 185.68$, $P < 0.001$ (interaction Contingency × Later Extinction Status: $F(1,17) = 0.00$, $P = 1.000$). Contingency awareness of the CS–US relationship was similarly reliable for the to-be extinguished (4-point scale: CS+E = 1.89 ± 0.47; CS–E = 0.28 ± 0.46; $t(17) = 8.79$, $P < 0.001$, one-sided) and to-be nonextinguished stimuli (CS+N = 1.83 ± 0.38; CS–N = 0.22 ± 0.43; $t(17) = 13.63$, $P < 0.001$, one-sided).

Table 1 Localization and statistics of the peak voxels of significant activations for fear conditioning and extinction within previously defined ROIs (one-sample *t*-tests and correlations with EEG Theta FER[b])

Experimental phase	Brain Structure	Side	MNI coordinates X	Y	Z	t_{max}	P_{FWE}
Day 1 Acquisition							
CS+ unpaired > CS–	Insula	L	–38	20	–4	5.14	0.035*
CS+ unpaired < CS–	vmPFC	L	–10	52	–2	5.34	0.055+
Day 1 Extinction							
CS+E > CS–E			–No significant results–				
CS+E < CS–E	Hippocampus	L	–32	–24	–14	7.24	<0.001**
	Hippocampus	R	32	–18	–14	5.13	0.014*
Day 2 fear and extinction recall test, parametric modulation to account for amygdala habituation[a]							
(CS+N – CS–N) > (CS+E – CS–E)	Amygdala	L	–20	–8	–12	4.66	0.015*
Positive correlation with EEG Theta FER[b]	Amygdala	R	32	0	–22	4.72	0.015*
(CS+N – CS–N) < (CS+E – CS–E)[c]			–No significant results–				

[a]Weighted with an exponentially decaying function to model amygdala habituation.

[b]EEG Theta FER = frontomedial (electrode Fz) theta fear and extinction recall assessed by the tetrad contrast (CS+N – CS–N) – (CS+E – CS–E).

[c]Note that correlations of this BOLD contrast with EEG Theta FER scores are not displayed separately, as these correlations are already covered by the correlations listed above. For example, a positive correlation of Theta FER scores with the contrast (CS+N – CS–N) > (CS+E – CS–E) is equivalent to a negative correlation with the contrast (CS+N – CS–N) < (CS+E – CS–E).

+$P_{FWE} \leq 0.10$, *$P_{FWE} \leq 0.05$, **$P_{FWE} \leq 0.01$ (ROI analyses, FWE-corrected according to SPM12 small volume correction, one peak per cluster is listed). All coordinates (X, Y, Z) are given in MNI space. L = left, R = right brain hemisphere.

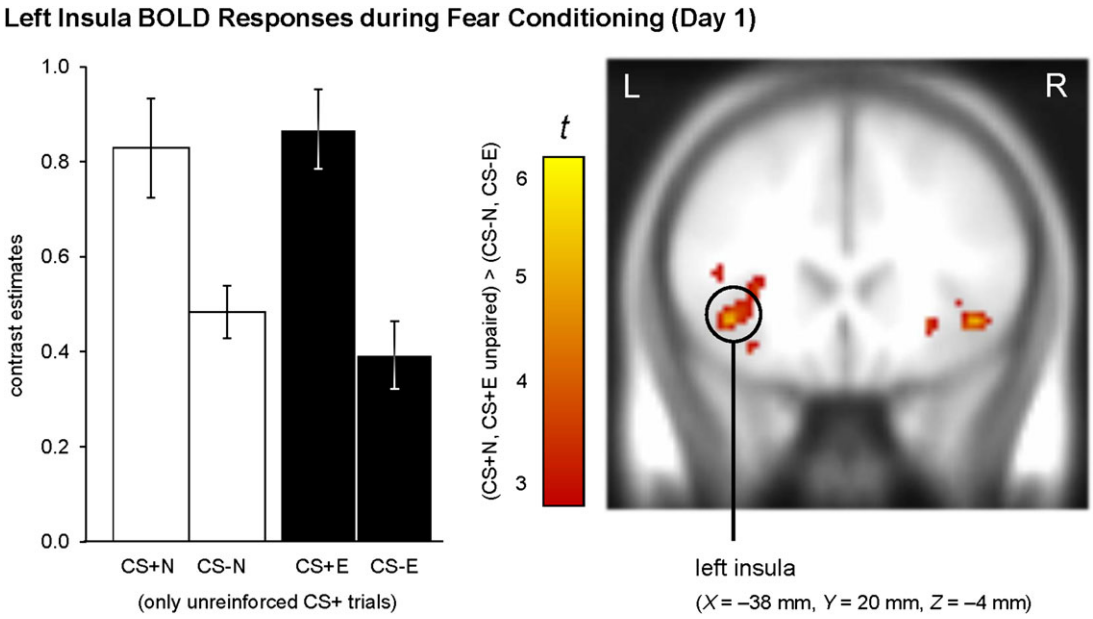

Figure 2. fMRI correlates of fear conditioning on Day 1. Insula activation was significantly enhanced for CS+ (CS+E, CS+N) compared with CS– (CS–E, CS–N). To confirm that neural responses did not differ between to-be extinguished and to-be nonextinguished stimuli, we constructed an additional first-level GLM which contained separate regressors for to-be extinguished and to-be nonextinguished CS+/CS–. Contrast estimates were extracted and subjected to a Contingency × Later Extinction Status ANOVA, which did not show a significant interaction, $F(1,17) = 0.65$, $P = 0.431$, but confirmed a significant main effect for Contingency, $F(1,17) = 24.45$, $P < 0.001$. For illustration purposes, the intensity threshold was set to $P \leq 0.005$ (uncorrected) with a minimal cluster threshold of $k \geq 5$ contiguous significant voxels. Activations (t-values) were superimposed on the MNI305 T1 template. All coordinates (X, Y, Z) are given in MNI space. L = left, R = right brain hemisphere. Bar graphs show the mean contrast estimates (±within-subject SEM, O'Brien and Cousineau 2014) for a cluster of voxels with $P \leq 0.005$ (uncorrected) surrounding the peak voxel within the insula ROI.

Collectively, these findings confirm successful fear conditioning at physiological and cognitive-affective levels. At the neural level, the left insula was the only region that was significantly more activated for CS+ versus CS– during the entire acquisition phase ($P_{FWE} = 0.035$, see Table 1 for statistical details). We confirmed that insula responses did not differ between to-be extinguished and to-be nonextinguished stimuli (Fig. 2).

Day 1 Fear Extinction

During subsequent Day 1 fear extinction, CS evoked SCRs showed a significant interaction of Contingency (CS+E vs. CS–E) and Time (beginning vs. end of extinction), $F(1,17) = 5.55$, $P = 0.031$. Participants showed higher SCRs for CS+E versus CS–E during the first 4 (Milad et al. 2013) extinction trials (CS+E = 0.16 ± 0.20; CS–E = 0.07 ± 0.11; $t(17) = 2.59$, $P = 0.010$, one-sided), indicating successful recall of conditioned fear at the beginning of the extinction session (Fig. 1C). Conversely, SCRs did not differ during the last 4 extinction trials (CS+E = 0.07 ± 0.12; CS–E = 0.06 ± 0.09; $t(17) = 0.14$, $P = 0.447$, one-sided), highlighting successful extinction learning. With respect to CS arousal ratings (Fig. 1D), a Contingency × Time (prior vs. after extinction) ANOVA revealed a significant main effect of Contingency, $F(1,17) = 5.17$, $P = 0.036$. As previously shown (Vansteenwegen et al. 2006), affective ratings remained relatively resistant against extinction throughout the entire extinction session. Differential arousal ratings were not reduced during extinction learning and indicated larger arousal ratings for CS+E versus CS–E both before (5-point scale: CS+E = 3.00 ± 0.91; CS–E = 2.44 ± 0.78; $t(17) = 1.97$, $P = 0.033$, one-sided) and after the extinction phase (5-point scale: CS+E = 2.94 ± 1.00; CS–E = 2.33 ± 0.84; $t(17) = 2.17$, $P = 0.023$, one-sided). For negative valence ratings (Fig. 1E), there was no significant effect of Contingency ($Ps \geq 0.104$). However, a significant effect of Time, $F(1,17) = 9.38$, $P = 0.007$, indicated a decline of ratings over time. Moreover, at the neural level, bilateral hippocampi were activated more strongly in response to CS–E versus CS+E throughout the entire extinction phase ($Ps_{FWE} \leq 0.014$, see Table 1).

Behavioral and SCR correlates of Day 2 Recall

While the Contingency × Extinction Status × Time interaction was only marginally significant with a two-sided test ($F(1,17) = 4.20$, $P = 0.056$; Fig. 1C), a planned contrast that reflected both habituation during recall and enhanced SCRs to CS+N versus all other stimuli (i.e., contrast values of 7, –1, –1, –1, … to CS+N, CS–N, CS+E, CS–E for the first and last 4 trials, respectively) was significant, $F(1,17) = 7.78$, $P = 0.013$. As expected, the nonextinguished previously conditioned fear-stimulus (CS+N = 0.18 ± 0.19) evoked larger SCRs than the nonextinguished CS– (CS–N = 0.09 ± 0.11; $t(17) = 2.10$, $P = 0.025$, one-sided) during the first 4 recall trials 24 h after conditioning and extinction, whereas there was no difference between CS+E (0.10 ± 0.17) and CS–E (0.11 ± 0.17) that had been presented during extinction, $t(17) = 0.30$, $P = 0.614$, one-sided (Fig. 1C). Moreover, there was no difference between CS+ and CS– during the last 4 recall trials for both extinguished (CS+E = 0.05 ± 0.07; CS–E = 0.05 ± 0.08; $t(17) = 0.002$, $P = 0.499$, one-sided) and nonextinguished stimuli (CS+N = 0.03 ± 0.06; CS–N = 0.05 ± 0.08; $t(17) = 1.08$, $P = 0.825$, one-sided). Furthermore, SCRs were larger during the first versus last 4 trials (main effect of Time, $F(1,17) = 5.04$, $P = 0.038$).

Moreover, similar to Day 1 extinction and in line with previous findings on extinction resistance of affective CS appraisal

(Vansteenwegen et al. 2006), both CS+ (5-point scale: CS+E = 3.03 ± 0.24; CS+N = 3.17 ± 0.20) stimuli were rated as significantly more arousing than both CS− stimuli (CS−E = 2.47 ± 0.20; CS−N = 2.39 ± 0.20) regardless of Day 1 extinction (Figure 1D; Contingency × Extinction Status × Time ANOVA; main effect of Contingency: $F(1,17) = 5.73$, $P = 0.029$; Contingency × Extinction Status interaction, $F(1,17) = 0.68$, $P = 0.420$). In addition to a main effect of Time, $F(1,17) = 7.56$, $P = 0.014$, the ANOVA on valence ratings did not show any significant main effects or interactions (Ps ≥ 0.101). Stimuli were rated as more negative at the beginning of Day 2 recall (Fig. 1E).

Electrophysiological Brain Correlates of Day 2 Recall

Replicating our prior human EEG study (Mueller et al. 2014b) and consistent with previous rodent work (Burgos-Robles et al. 2009), a significant Contingency × Extinction Status interaction, $F(1,17) = 6.88$, $P = 0.018$, revealed that differential (CS+ vs. CS−) frontomedial theta power was significantly reduced for extinguished versus nonextinguished stimuli (Fig. 3A). Moreover, we observed higher theta power for CS+N compared with CS−N, $t(17) = 2.31$, $P = 0.017$, one-sided, whereas there was no difference in theta power between extinguished stimuli CS+E and

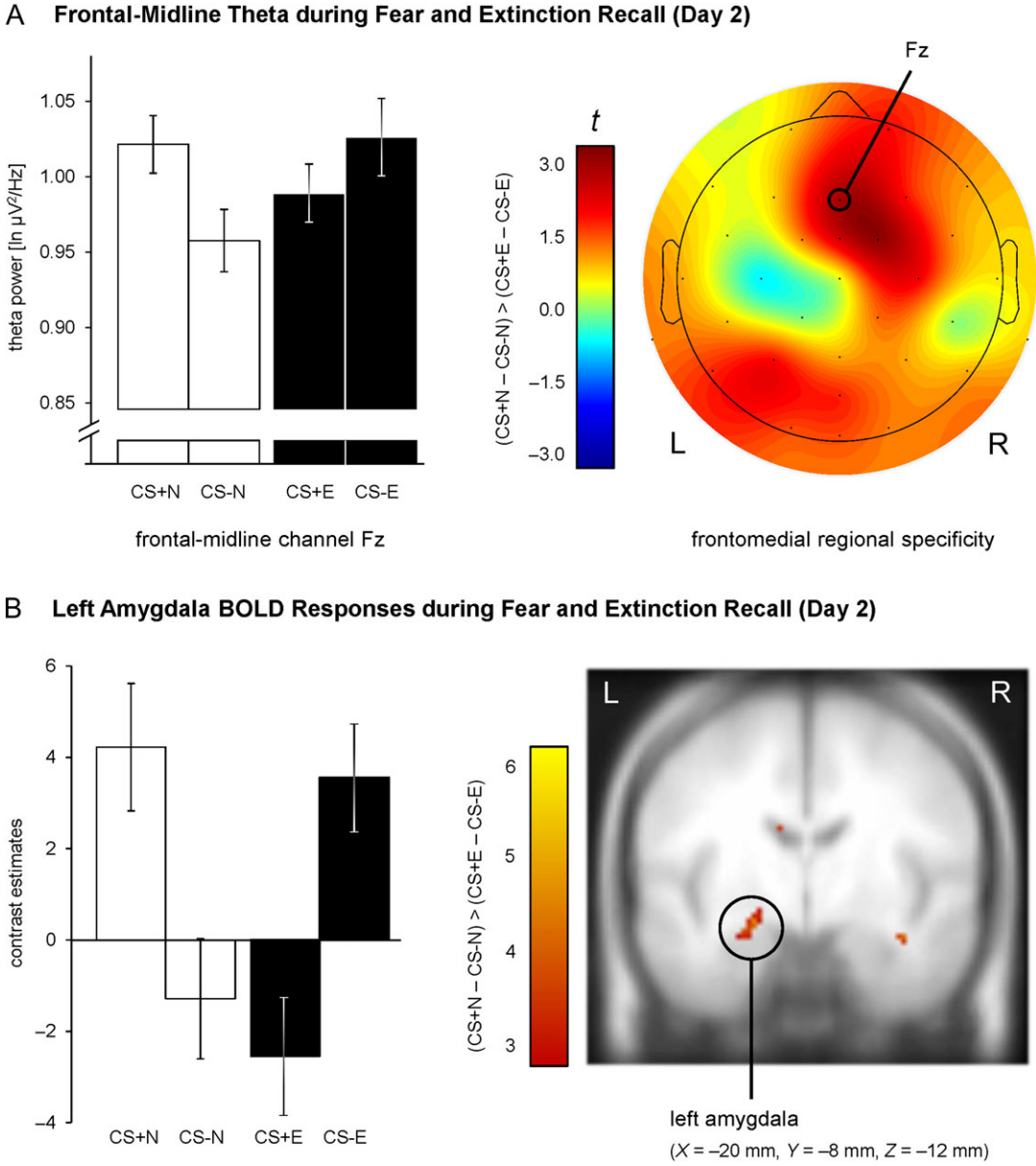

Figure 3. EEG and fMRI correlates of fear and extinction recall on Day 2. (*A*) Differential (CS+ – CS−) ln-transformed theta power at frontal-midline channel Fz was significantly reduced for extinguished versus nonextinguished stimuli (left). This effect was specific for frontomedial electrode channels (right). Bar graphs show the mean theta power (± within-subject SEM, O'Brien and Cousineau 2014). (*B*) Reduced differential amygdala responses (CS+ – CS−) for extinguished compared with nonextinguished stimuli. Habituation of amygdala activity was modeled by an exponentially decaying function, based on habituation of SCRs. For illustration purposes, the intensity threshold was set to $P \leq 0.005$ (uncorrected) with a minimal cluster threshold of $k \geq 5$ contiguous significant voxels. Activations (*t*-values) were superimposed on the MNI305 T1 template. All coordinates (X, Y, Z) are given in MNI space. L = left, R = right brain hemisphere. Bar graphs show the mean contrast estimates (± within-subject SEM, O'Brien and Cousineau 2014) for a cluster of voxels with $P \leq 0.005$ (uncorrected) surrounding the peak voxel within the amygdala ROI.

CS−E, $t(17) = 1.11$, $P = 0.859$, one-sided. Highlighting the specific role of frontomedial oscillations within the theta frequency band for fear expression (Mueller et al. 2014b), this effect showed a frontomedial topography (Fig. 3A) and was constrained to the theta frequency band (delta, 1–4 Hz: $P = 0.334$; alpha, 8–13 Hz: $P = 0.074$; beta, 13–30 Hz: $P = 0.242$).

Hemodynamic Brain Correlates of Day 2 Recall

During Day 2 recall, differential BOLD responses were significantly reduced for extinguished versus nonextinguished stimuli, that is [(CS+N − CS−N) > (CS+E − CS−E)], in the left amygdala (peak voxel in MNI space: $X = -20$ mm, $Y = -8$ mm, $Z = -12$ mm), indicating successful recall of conditioned and extinguished fear in this putative hub region of the fear network ($P_{FWE} = 0.015$, see Table 1 and Fig. 3B). A more detailed analysis of the activation time course (see Supplementary Material E) confirmed that this complex contrast of regressors, which were modeled by an exponentially decaying function, was primarily driven by increased amygdala activation to CS+N − CS−N (reflecting successful fear recall), and decreased amygdala activation to CS+E − CS−E (reflecting successful extinction recall) during the first trials of the recall phase, which diminished over time.

Reduced differential BOLD responses for extinguished versus nonextinguished stimuli was replicated in the bilateral amygdalae (left peak voxel: $X = -26$ mm, $Y = -8$ mm, $Z = -18$ mm; right peak voxel: $X = 30$ mm, $Y = -6$ mm, $Z = -20$ mm) when the analysis was restricted to the first 4 recall trials as in Milad et al. (2007b) ($Ps_{FWE} \leq 0.043$, Supplementary Material F, see Supplementary Table S1 for statistical details).

Integration of Electrophysiological and Hemodynamic Brain Correlates of Day 2 Recall

To investigate putative relations between EEG and fMRI data, a score reflecting the degree of differential modulation to nonextinguished versus extinguished conditioned stimuli [FER = (CS+N − CS−N) − (CS+E − CS−E)] was computed for theta power at frontal-midline channel Fz and entered as a covariate in second-level simple regression analysis. This analysis revealed a positive correlation between theta EEG FER and right amygdala (peak voxel in MNI space: $X = 32$ mm, $Y = 0$ mm, $Z = -22$ mm) BOLD FER modulation ($P_{FWE} = 0.015$, see Fig. 4 and Table 1). This indicates that high recall of conditioned and extinguished fear for EEG theta power (high FER theta scores) was associated with high FER for fMRI amygdala activation (high FER BOLD scores). Notably, 60% of the variance for the FER contrast was shared by theta oscillations and amygdala activation ($R^2 = 0.60$).

A trend for a similar theta-amygdala correlation for the FER contrast emerged ($P = 0.087$) when fMRI analysis was restricted to the first 4 (Milad et al. 2007b) recall trials (Supplementary Material F, see Supplementary Table S1). In addition, a negative correlation ($P = 0.038$) of theta EEG and vmPFC BOLD modulation emerged (Supplementary Material F, see Supplementary Fig. S5), consistent with a putative inhibitory role of the vmPFC on fear expression during early extinction recall (for a review, Milad and Quirk 2012).

The described covariation between theta power and amygdala activation is based on covariation of FER scores, which represent a combination of recall of conditioned and extinguished fear. Thus, it remains unclear whether this correlation of FER scores reflects covariation of fear-related (CS+N vs. CS−N) or extinction-related (CS+E vs. CS−E) effects. To disentangle these important alternative explanations, multivariate regression and univariate follow-up analyses were performed (Supplementary Material G). These analyses revealed that fear-related EEG theta modulations (CS+N − CS−N) negatively predicted extinction-related fMRI amygdala responses (CS+E − CS−E, $\beta = -0.74$, $P = 0.001$; Supplementary Material G, see Supplementary Table S2 for statistical details).

Discussion

Translating insights from rodent threat processing studies to human brains is both challenging and important, as assumed functional and structural homologies are controversial (Heilbronner et al. 2016). The primary goal of this study was to investigate the relationship between frontal theta oscillations and amygdala activation in the human brain, with emphasis on its specific role for fear and extinction memory. Therefore, we integrated (1) frontomedial theta oscillations during expression of conditioned fear and fear extinction, as previously revealed in human EEG and rodent studies, and (2) fear and extinction networks identified by fMRI in humans. Specifically, we recorded 31-channel EEG and fMRI simultaneously during a 24 h-delayed recall of previously conditioned as well as extinguished fear. As hypothesized, nonextinguished stimuli evoked stronger differential (CS+ vs. CS−) frontomedial oscillatory theta activity (EEG) and amygdala BOLD responses (fMRI) than extinguished stimuli. Furthermore, FER effects on EEG theta power covaried with amygdala responses, demonstrating for the first time that human frontomedial theta is linked to amygdala activation during threat processing, as previously observed in rodent studies (Gilmartin et al. 2014).

Successful fear conditioning on Day 1 could be shown at the psychophysiological (autonomic nervous system), subjective (arousal/valence), and neural (insula) level. Consistent with successful fear extinction, differential SCRs decreased during the extinction procedure and remained diminished even 24 h later. Similar to prior studies, bilateral hippocampal activation was increased for CS−E vs. CS+E during extinction learning, which was previously interpreted as indexing the development of an extinction memory trace (Phelps et al. 2004; Milad and Quirk 2012; Merz et al. 2014).

Replicating previous findings in humans (Mueller et al. 2014b) and in animals (Burgos-Robles et al. 2009; Gilmartin et al. 2014), extinction learning reduced differential frontal-midline theta power during extinction recall 24 h later. There is strong evidence from animal studies that medial frontal theta plays a critical role during sustained fear expression (Burgos-Robles et al. 2009) and extinction (Lesting et al. 2013). Complementing these animal findings, frontal-midline theta has also been linked to processing of fear and anxiety in humans (Mitchell et al. 2008; Mueller et al. 2014b; Cavanagh and Shackman 2015). Source-localization studies using EEG and MEG in humans have revealed that the AMC is the predominant generator for frontal-midline theta, which shows a reliable maximum at electrode Fz on the scalp level (Mitchell et al. 2008; Mueller et al. 2014b). Moreover, AMC-localized EEG activity is a predictor for subsequent heart rate changes (Panitz et al. 2013) with relevance for conditioned fear (Panitz et al. 2015). Collectively, these findings raise the possibility that AMC-mediated frontal-midline theta may play a crucial role in carrying out adaptive changes during fear expression (Cavanagh and Shackman 2015).

Mirroring findings involving theta oscillations, extinction training on Day 1 also reduced differential amygdala BOLD responses during Day 2 recall. While previous fMRI studies

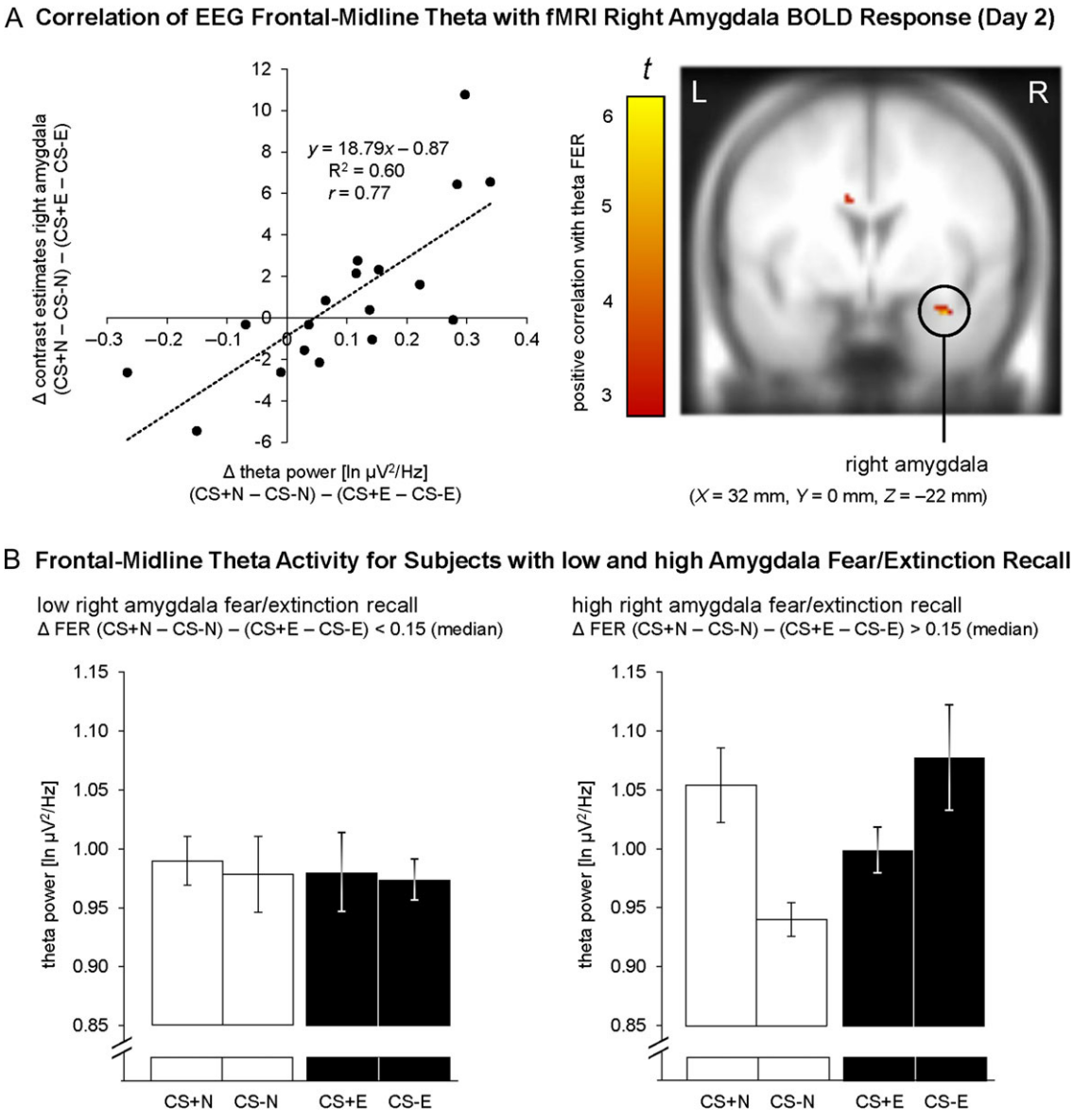

Figure 4. Integration of EEG frontomedial (Fz) theta power and fMRI right amygdala activation of fear and extinction recall on Day 2. (*A*) Positive correlation of theta modulations to conditioned and extinguished fear with BOLD responses in the right amygdala. Consistent with our assumed involvement of theta oscillations in AMC-amygdala connectivity (Gilmartin et al. 2014), this correlation indicates that subjects with relatively strong amygdala activation to nonextinguished (vs. extinguished) fear stimuli are characterized by relatively strong differential frontomedial theta power. For illustration purposes, the intensity threshold was set to $P \leq 0.005$ (uncorrected) with a minimal cluster threshold of $k \geq 5$ contiguous significant voxels. Activations (*t*-values) were superimposed on the MNI305 T1 template. All coordinates (X, Y, Z) are given in MNI space. L = left, R = right brain hemisphere. (*B*) To illustrate the positive correlation, right amygdala BOLD responses for the FER contrast (CS+N – CS–N) – (CS+E – CS–E) were compared based on median split, and theta power was assessed separately for subjects with low and high amygdala fear/extinction recall, that is, low/high FER BOLD scores (bar graphs show $M \pm$ within-subject SEM, O'Brien and Cousineau 2014). Higher differential theta power for nonextinguished versus extinguished CSs only emerged for subjects with high ($P < 0.001$), but not with low ($P = 0.929$) fear/extinction recall in the right amygdala.

have shown reduced amygdala activation to a previously extinguished CS+ compared with a CS– (Phelps et al. 2004; Hermann et al. 2016), the present study is the first to demonstrate that differential amygdala activation is significantly reduced for extinguished as compared with nonextinguished CS+ versus CS– stimulus pairs. Diminished amygdala activation during extinction recall may reflect processing of altered input about the predictive value of the CS+ (Phelps et al. 2004) and/or it may indicate a suppression of fear expression (Quirk and Mueller 2008), possibly through reduced afferent activity from the AMC (Vertes 2004) and/or increased inhibitory activity via connections from vmPFC to intercalated cells (Quirk and Mueller 2008; Pitman et al. 2012). This pattern of results is supported by animal findings suggesting that activity of fear-initiating amygdala neurons is "switched off" (Quirk and Mueller 2008) during the retrieval of extinction memories.

Importantly, the pattern of EEG theta power closely mirrored fMRI amygdala responses. Moreover, the differentiation between extinguished versus nonextinguished conditioned responses as measured by frontomedial theta scaled with the differentiation between extinguished and nonextinguished conditioned responses within the right amygdala. Notably, 60% of the variance in differential theta power could be explained by variation in differential amygdala BOLD responses. In particular, fear-related EEG theta

responses to nonextinguished stimuli covaried with fMRI amygdala activation to extinguished stimuli. This pattern was consistent with univariate analyses, where the Contingency × Extinction interaction on theta was primarily driven by nonextinguished CSs (mirroring Mueller et al. 2014b), whereas the Contingency × Extinction interaction on right amygdala was primarily driven by extinguished CSs (mirroring Phelps et al. 2004 and Hermann et al. 2016). This may reflect that communication within the fear and extinction network is modulated by synchronized theta oscillations (Bocchio and Capogna 2014; Gilmartin et al. 2014). In mice, theta synchronicity between the medial prefrontal cortex and the amygdala has been associated with better discrimination between CS+ and CS− after fear conditioning (Likhtik et al. 2014). Thus, our findings may reflect altered communication between the amygdala and prefrontal cortex (Likhtik and Gordon 2014) during the processing of threat-signaling stimuli that have not been subject to extinction.

As described above, the correlation with theta oscillations for fear compared with extinction recall was only evident for the right amygdala. Correlations between amygdala activation and other behavioral and physiological conditioned responses are often driven by the right amygdala (LaBar et al. 1998; Phelps et al. 2001, 2004) and right amygdala activation is particularly involved when the US elicits an immediate aversive response (Phelps et al. 2001), which might be particularly the case with electric shocks (LaBar et al. 1998). The present results suggest that immediate processing of aversive stimuli varied across participants, and that aversive responses generated by the right amygdala may be subject to top-down regulation by medial frontal theta oscillations emanating from the AMC (Gilmartin et al. 2014).

Taken together, our findings suggest that amygdala activation and AMC theta oscillations are both influenced by fear conditioning and extinction learning and that they covary with each other. Two routes are possible to explain functional coupling between both brain areas. First, the amygdala, as a hub for fear-related processes, may send efferent output during CS presentation to modulate the salience of the CS after extinction learning (Gilmartin et al. 2014; Senn et al. 2014). The AMC may then integrate these amygdaloid afferents with temporal and contextual information retrieved from other brain circuits (Fuster 2001; Gilmartin et al.2014). Second, reduced excitatory projections from the AMC back to the amygdala (Gilmartin et al. 2014) are presumed to come along with reduced theta synchrony (Bocchio and Capogna 2014). In the end, these projections may suppress amygdala-mediated fear responses (Pitman et al. 2012), signaling a reduced predictive value of the CS (Courtin et al. 2014; Gilmartin et al. 2014). Consistent with this second model, animal studies have shown that prelimbic theta input is crucial to reduce firing of amygdala neurons during safety (Likhtik et al. 2014), highlighting a dominant role of AMC theta for both fear and extinction learning (Quirk and Mueller 2008; Bocchio and Capogna 2014). In addition to the amygdala, the AMC may receive inhibitory inputs from the vmPFC, which is involved in extinction recall (Milad et al. 2007b; Hermann et al. 2016) and in the current study was negatively correlated with frontomedial theta (Supplementary Material F).

Some limitations of the study should be noted. First, in order to achieve an adequate signal-to-noise ratio for EEG recordings, it was necessary to include more trials than typically used in neuroimaging studies on fear conditioning and extinction (Fullana et al. 2016). Also, because BOLD responses in the amygdala have been found to show a rapid habituation after repeated CS presentations (Büchel et al. 1998), recall trials were weighted with an exponentially decaying function for the fMRI analysis (Büchel et al. 1998; Armony and Dolan 2001) but not the EEG analysis. Further, we implemented a complementary analytic approach that focused on only the first 4 fMRI trials (e.g., as in Milad et al. 2007b). Though this approach does not resolve the asymmetry of fMRI and EEG analyses, a very similar pattern of results emerged (see Supplementary Material F). Second, while the AMC is thought to be the predominant generator for frontal-midline theta oscillations (Mitchell et al. 2008; Mueller et al. 2014b), reduced differential EEG theta power was not accompanied by reduced differential AMC BOLD responses in our data. Fluctuations of the BOLD signal are challenging to directly map onto EEG power effects (Fellner et al. 2016). Although changes in EEG and fMRI signals are both correlated with local field potentials (Logothetis et al. 2001; Buzsáki, Anastassiou, Koch 2012; Herreras 2016), they may relate to different neural processes (Ekstrom 2010; Lopes da Silva 2013; Jorge, van der Zwaag, Figueiredo 2014), and the co-occurrence of multiple underlying physiological mechanisms is of particular relevance for measurable prefrontal brain correlates during threat processing (Etkin, Egner, Kalisch 2011; Delgado et al. 2016). Furthermore, it should be kept in mind that fear conditioning studies vary in the type of conditioned/unconditioned stimuli, number of trials, CS–US reinforcement rate, and CS–US delay, which seems to affect the degree with which AMC BOLD effects can be detected (Fullana et al. 2016). Third, the spatial resolution of noninvasive imaging methods used in humans, including fMRI, is limited (Keifer et al. 2015). In the present study, we found reduced differential amygdala activation after extinction training suggesting that measured amygdala activation was coding for the level of fear (Amano et al. 2011). Research in animals highlights the coexistence of both fear and extinction coding cells in the amygdala, with reciprocal patterns of activity (Quirk and Mueller 2008). To gain a better understanding of specific contributions of small adjacent subnuclei, connectivity of fear and extinction circuits within the amygdala with AMC theta oscillations should further be explored in animals.

Despite these limitations, this study demonstrated that simultaneous EEG–fMRI can capture oscillatory (theta) and subcortical (amygdala) fear-related activity at the same time in the human brain. With this approach, we linked animal-based findings on frontal theta to amygdala activity in humans. These findings lay the foundation for studying abnormal fear processing in psychopathology (Bowers and Ressler 2015). Given that current models imply exaggerated amygdala responses and deficient prefrontal functioning in patients with anxiety disorders (Bruhl et al. 2014; Rauch, Shin, Phelps 2006), investigations focusing on theta oscillations promise to be particularly important for probing disrupted communication among key nodes within the fear system. This knowledge might, in turn, open new avenues for treatment in anxiety and related disorders.

Authors' Contributions

M.F.J.S., C.P., A.H., C.H., D.A.P., and E.M.M. conceived and designed the study. M.F.J.S. and C.P. acquired the data. M.F.J.S., C.P., I.M.R., D.G.D., P.K., A.H., A.E.W., D.A.P., and E.M.M. analyzed the data. M.F.J.S., D.A.P., and E.M.M. drafted the article. All of the authors interpreted the data, discussed the results, and commented on the article.

Supplementary Material

Supplementary material is available at *Cerebral Cortex* online.

Funding

This work was supported by a Grant from the Deutsche Forschungsgemeinschaft (grant number DFG MU3535/2-3) to E. M.M.; by a grant from the Justus Liebig University Giessen (Germany) to E.M.M; by a PROMOS scholarship of the German Academic Exchange Service (DAAD) to M.F.J.S.; and by the Young Researcher Award of the World Association for Stress Related and Anxiety Disorders (WASAD) to M.F.J.S. Over the past 3 years, D.A.P. received consulting fees from Akili Interactive Labs, BlackThorn Therapeutics, Boehringer Ingelheim, Pfizer, and Posit Science, for activities unrelated to the current research. NIH (grant R37 MH068376 to D.A.P.: partially supported). NIH (grant R01 MH096987 to I.M.R.: partially supported). In the last 3 years, D.G.D. has served as a consultant for Pfizer on unrelated projects. NIH (grant 4R00MH094438-03 to D.G.D.), DFG (grant MU3535/2 -3 to M.F.J.S.), and DFG (grant MU3535/2-1 to C.P.).

Notes

We would like to thank Gebhard Sammer and Helge Gebhardt (Center for Psychiatry, University of Giessen, Germany) for providing artifact removal pipelines for EEG data. We also wish to thank Kerry J. Ressler (Neurobiology of Fear Laboratory, McLean Hospital, Harvard Medical School, MA, USA) for valuable discussions on the project and on linking our results to previous findings from animal models research. Further, we thank Carlo R. Blecker (Bender Institute of Neuroimaging, University of Giessen, Germany) for technical assistance. Address correspondence to Matthias F.J. Sperl, Department of Psychology, Personality Psychology and Assessment, University of Marburg, 35032 Marburg, Germany. Email: matthias.sperl@staff.uni-marburg.de. *Conflict of Interest*: None declared.

References

Allen PJ, Josephs O, Turner R. 2000. A method for removing imaging artifact from continuous EEG recorded during functional MRI. NeuroImage. 12:230–239.

Allen PJ, Polizzi G, Krakow K, Fish DR, Lemieux L. 1998. Identification of EEG events in the MR scanner: the problem of pulse artifact and a method for its subtraction. NeuroImage. 8:229–239.

Amano T, Duvarci S, Popa D, Pare D. 2011. The fear circuit revisited: contributions of the basal amygdala nuclei to conditioned fear. J Neurosci. 31:15481–15489.

Armony JL, Dolan RJ. 2001. Modulation of auditory neural responses by a visual context in human fear conditioning. Neuroreport. 12:3407–3411.

Bastiaansen M, Mazaheri A, Jesen O. 2012. Beyond ERPs: oscillatory neuronal dynamics. In: Luck SJ, Kappenman ES, editors. The Oxford handbook of event-related potential components. New York, NY: Oxford University Press. p. 31–49.

Bocchio M, Capogna M. 2014. Oscillatory substrates of fear and safety. Neuron. 83:753–755.

Bowers ME, Ressler KJ. 2015. An overview of translationally informed treatments for posttraumatic stress disorder: animal models of Pavlovian fear conditioning to human clinical trials. Biol Psychiatry. 78:E15–E27.

Brett M, Anton J-L, Valabregue R, Poline J-B. 2002. Region of interest analysis using an SPM toolbox. NeuroImage. 16: Supplement1. Available on CD-ROM.

Bruhl AB, Delsignore A, Komossa K, Weidt S. 2014. Neuroimaging in social anxiety disorder—a meta-analytic review resulting in a new neurofunctional model. Neurosci Biobehav Rev. 47:260–280.

Büchel C, Dolan RJ, Armony JL, Friston KJ. 1999. Amygdala-hippocampal involvement in human aversive trace conditioning revealed through event-related functional magnetic resonance imaging. J Neurosci. 19:10869–10876.

Büchel C, Morris J, Dolan RJ, Friston KJ. 1998. Brain systems mediating aversive conditioning: an event-related fMRI study. Neuron. 20:947–957.

Burgos-Robles A, Vidal-Gonzalez I, Quirk GJ. 2009. Sustained conditioned responses in prelimbic prefrontal neurons are correlated with fear expression and extinction failure. J Neurosci. 29:8474–8482.

Buzsáki G, Anastassiou CA, Koch C. 2012. The origin of extracellular fields and currents—EEG, ECoG, LFP and spikes. Nat Rev Neurosci. 13:407–420.

Cavanagh JF, Shackman AJ. 2015. Frontal midline theta reflects anxiety and cognitive control: meta-analytic evidence. J Physiol Paris. 109:3–15.

Courtin J, Chaudun F, Rozeske RR, Karalis N, Gonzalez-Campo C, Wurtz H, Abdi A, Baufreton J, Bienvenu TCM, Herry C. 2014. Prefrontal parvalbumin interneurons shape neuronal activity to drive fear expression. Nature. 505:92–96.

Delgado MR, Beer JS, Fellows LK, Huettel SA, Platt ML, Quirk GJ, Schiller D. 2016. Viewpoints: dialogues on the functional role of the ventromedial prefrontal cortex. Nat Neurosci. 19: 1545–1552.

Diekhof EK, Geier K, Falkai P, Gruber O. 2011. Fear is only as deep as the mind allows: a coordinate-based meta-analysis of neuroimaging studies on the regulation of negative affect. NeuroImage. 58:275–285.

Ekman P, Friesen WV. 1976. Pictures of facial affect. Palo Alto (CA): Consulting Psychologists.

Ekstrom A. 2010. How and when the fMRI BOLD signal relates to underlying neural activity: the danger in dissociation. Brain Res Rev. 62:233–244.

Etkin A, Egner T, Kalisch R. 2011. Emotional processing in anterior cingulate and medial prefrontal cortex. Trends Cogn Sci. 15:85–93.

Fellner M-C, Volberg G, Wimber M, Goldhacker M, Greenlee MW, Hanslmayr S. 2016. Spatial mnemonic encoding: theta power decreases and medial temporal lobe BOLD increases co-occur during the usage of the method of loci. eNeuro. 3: 0184–16.2016.

Fullana MA, Harrison BJ, Soriano-Mas C, Vervliet B, Cardoner N, Avila-Parcet A, Radua J. 2016. Neural signatures of human fear conditioning: an updated and extended meta-analysis of fMRI studies. Mol Psychiatry. 21:500–508.

Fuster JM. 2001. The prefrontal cortex—an update. Neuron. 30: 319–333.

Gilmartin MR, Balderston NL, Helmstetter FJ. 2014. Prefrontal cortical regulation of fear learning. Trends Neurosci. 37: 455–464.

Goosens KA, Maren S. 2004. NMDA receptors are essential for the acquisition, but not expression, of conditional fear and associative spike firing in the lateral amygdala. Eur J Neurosci. 20:537–548.

Hartley CA, Phelps EA. 2009. Changing fear: the neurocircuitry of emotion regulation. Neuropsychopharmacology. 35:136–146.

Heilbronner SR, Rodriguez-Romaguera J, Quirk GJ, Groenewegen HJ, Haber SN. 2016. Circuit-based corticostriatal homologies between rat and primate. Biol Psychiatry. 80:509–521.

Hermann A, Keck T, Stark R. 2014. Dispositional cognitive reappraisal modulates the neural correlates of fear acquisition and extinction. Neurobiol Learn Mem. 113:115–124.

Hermann A, Schäfer A, Walter B, Stark R, Vaitl D, Schienle A. 2009. Emotion regulation in spider phobia: role of the medial prefrontal cortex. Soc Cogn Affect Neurosci. 4:257–267.

Hermann A, Stark R, Milad MR, Merz CJ. 2016. Renewal of conditioned fear in a novel context is associated with hippocampal activation and connectivity. Soc Cogn Affect Neurosci. 11:1411–1421.

Hermans EJ, Kanen JW, Tambini A, Fernández G, Davachi L, Phelps EA. 2017. Persistence of amygdala-hippocampal connectivity and multi-voxel correlation structures during awake rest after fear learning predicts long-term expression of fear. Cereb Cortex. 27:3028–3041.

Herreras O. 2016. Local field potentials: myths and misunderstandings. Front Neural Circuits. 10:101.

Hwang MJ, Zsido RG, Song H, Pace-Schott EF, Miller KK, Lebron-Milad K, Marin M-F, Milad MR. 2015. Contribution of estradiol levels and hormonal contraceptives to sex differences within the fear network during fear conditioning and extinction. BMC Psychiatry. 15:295.

Janak PH, Tye KM. 2015. From circuits to behaviour in the amygdala. Nature. 517:284–292.

Jorge J, van der Zwaag W, Figueiredo P. 2014. EEG-fMRI integration for the study of human brain function. NeuroImage. 102:24–34.

Kalisch R, Korenfeld E, Stephan KE, Weiskopf N, Seymour B, Dolan RJ. 2006. Context-dependent human extinction memory is mediated by a ventromedial prefrontal and hippocampal network. J Neurosci. 26:9503–9511.

Keifer OP JR, Hurt RC, Ressler KJ, Marvar PJ. 2015. The physiology of fear: reconceptualizing the role of the central amygdala in fear learning. Physiology (Bethesda). 30:389–401.

Kim WB, Cho J-H. 2017. Encoding of discriminative fear memory by input-specific LTP in the amygdala. Neuron. 95:1129–1146.e5.

Kim JJ, Jung MW. 2006. Neural circuits and mechanisms involved in Pavlovian fear conditioning: a critical review. Neurosci Biobehav Rev. 30:188–202.

Klimesch W. 1996. Memory processes, brain oscillations and EEG synchronization. Int J Psychophysiol. 24:61–100.

Knight DC, Nguyen HT, Bandettini PA. 2005. The role of the human amygdala in the production of conditioned fear responses. NeuroImage. 26:1193–1200.

LaBar KS, Gatenby JC, Gore JC, LeDoux JE, Phelps EA. 1998. Human amygdala activation during conditioned fear acquisition and extinction: a mixed-trial fMRI study. Neuron. 20: 937–945.

LeDoux JE. 2014. Coming to terms with fear. Proc Natl Acad of Sci USA. 111:2871–2878.

Lesting J, Daldrup T, Narayanan V, Himpe C, Seidenbecher T, Pape H-C. 2013. Directional theta coherence in prefrontal cortical to amygdalo-hippocampal pathways signals fear extinction. PLoS One. 8:e77707.

Likhtik E, Gordon JA. 2014. Circuits in sync: decoding theta communication in fear and safety. Neuropsychopharmacology. 39:235–236.

Likhtik E, Stujenske JM, Topiwala MA, Harris AZ, Gordon JA. 2014. Prefrontal entrainment of amygdala activity signals safety in learned fear and innate anxiety. Nat Neurosci. 17: 106–113.

Lingawi NW, Westbrook RF, Laurent V. 2016. Extinction and latent inhibition involve a similar form of inhibitory learning that is stored in and retrieved from the infralimbic cortex. Cereb Cortex. 27:5547–5556.

Logothetis NK, Pauls J, Augath M, Trinath T, Oeltermann A. 2001. Neurophysiological investigation of the basis of the fMRI signal. Nature. 412:150–157.

Lonsdorf TB, Menz MM, Andreatta M, Fullana MA, Golkar A, Haaker J, Heitland I, Hermann A, Kuhn M, Kruse O, et al. 2017. Don't fear 'fear conditioning': methodological considerations for the design and analysis of studies on human fear acquisition, extinction, and return of fear. Neurosci Biobehav Rev. 77:247–285.

Lopes da Silva F. 2013. EEG and MEG: relevance to neuroscience. Neuron. 80:1112–1128.

Lykken DT, Venables PH. 1971. Direct measurement of skin conductance: a proposal for standardization. Psychophysiology. 8:656–672.

Margraf J. 1994. MINI-DIPS: Diagnostisches Kurz-Interview bei psychischen Störungen (Diagnostic interview for mental disorders—short version). Berlin (Germany): Springer.

Merz CJ, Hermann A, Stark R, Wolf OT. 2014. Cortisol modifies extinction learning of recently acquired fear in men. Soc Cogn Affect Neurosci. 9:1426–1434.

Milad MR, Furtak SC, Greenberg JL, Keshaviah A, Im JJ, Falkenstein MJ, Jenike M, Rauch SL, Wilhelm S. 2013. Deficits in conditioned fear extinction in obsessive-compulsive disorder and neurobiological changes in the fear circuit. JAMA Psychiatry. 70:608.

Milad MR, Pitman RK, Ellis CB, Gold AL, Shin LM, Lasko NB, Zeidan MA, Handwerger K, Orr SP, Rauch SL. 2009. Neurobiological basis of failure to recall extinction memory in posttraumatic stress disorder. Biol Psychiatry. 66:1075–1082.

Milad MR, Quirk GJ. 2012. Fear extinction as a model for translational neuroscience: ten years of progress. Annu Rev Psychol. 63:129–151.

Milad MR, Quirk GJ, Pitman RK, Orr SP, Fischl B, Rauch SL. 2007a. A role for the human dorsal anterior cingulate cortex in fear expression. Biol Psychiatry. 62:1191–1194.

Milad MR, Wright CI, Orr SP, Pitman RK, Quirk GJ, Rauch SL. 2007b. Recall of fear extinction in humans activates the ventromedial prefrontal cortex and hippocampus in concert. Biol Psychiatry. 62:446–454.

Mitchell DJ, McNaughton N, Flanagan D, Kirk IJ. 2008. Frontal-midline theta from the perspective of hippocampal "theta". Prog Neurobiol. 86:156–185.

Mizuseki K, Sirota A, Pastalkova E, Buzsáki G. 2009. Theta oscillations provide temporal windows for local circuit computation in the entorhinal-hippocampal loop. Neuron. 64: 267–280.

Mueller EM, Burgdorf C, Chavanon M-L, Schweiger D, Wacker J, Stemmler G. 2014a. Dopamine modulates frontomedial failure processing of agentic introverts versus extraverts in incentive contexts. Cogn Affect Behav Neurosci. 14:756–768.

Mueller EM, Panitz C, Hermann C, Pizzagalli DA. 2014b. Prefrontal oscillations during recall of conditioned and extinguished fear in humans. J Neurosci. 34:7059–7066.

Narayanan V, Heiming RS, Jansen F, Lesting J, Sachser N, Pape H-C, Seidenbecher T. 2011. Social defeat: impact on fear extinction and amygdala-prefrontal cortical theta synchrony in 5-HTT deficient mice. PLoS One. 6:e22600.

O'Brien F, Cousineau D. 2014. Representing error bars in within-subject designs in typical software packages. Quant Methods Psychol. 10:56–67.

Panitz C, Hermann C, Mueller EM. 2015. Conditioned and extinguished fear modulate functional corticocardiac coupling in humans. Psychophysiology. 52:1351–1360.

Panitz C, Wacker J, Stemmler G, Mueller EM. 2013. Brain-heart coupling at the P300 latency is linked to anterior cingulate cortex and insula—a cardio-electroencephalographic covariance tracing study. Biol Psychol. 94:185–191.

Pejic T, Hermann A, Vaitl D, Stark R. 2013. Social anxiety modulates amygdala activation during social conditioning. Soc Cogn Affect Neurosci. 8:267–276.

Phelps EA, Delgado MR, Nearing KI, LeDoux JE. 2004. Extinction learning in humans: role of the amygdala and vmPFC. Neuron. 43:897–905.

Phelps EA, LeDoux JE. 2005. Contributions of the amygdala to emotion processing: from animal models to human behavior. Neuron. 48:175–187.

Phelps EA, O'Connor KJ, Gatenby JC, Gore JC, Grillon C, Davis M. 2001. Activation of the left amygdala to a cognitive representation of fear. Nat Neurosci. 4:437–441.

Pineles SL, Orr MR, Orr SP. 2009. An alternative scoring method for skin conductance responding in a differential fear conditioning paradigm with a long-duration conditioned stimulus. Psychophysiology. 46:984–995.

Pitman RK, Rasmusson AM, Koenen KC, Shin LM, Orr SP, Gilbertson MW, Milad MR, Liberzon I. 2012. Biological studies of post-traumatic stress disorder. Nat Rev Neurosci. 13: 769–787.

Quirk GJ, Mueller D. 2008. Neural mechanisms of extinction learning and retrieval. Neuropsychopharmacology. 33:56–72.

Quirk GJ, Repa C, LeDoux JE. 1995. Fear conditioning enhances short-latency auditory responses of lateral amygdala neurons: parallel recordings in the freely behaving rat. Neuron. 15:1029–1039.

Rauch SL, Shin LM, Phelps EA. 2006. Neurocircuitry models of posttraumatic stress disorder and extinction: human neuroimaging research—past, present, and future. Biol Psychiatry. 60: 376–382.

Repa JC, Muller J, Apergis J, Desrochers TM, Zhou Y, LeDoux JE. 2001. Two different lateral amygdala cell populations contribute to the initiation and storage of memory. Nat Neurosci. 4:724–731.

Sammer G, Blecker C, Gebhardt H, Kirsch P, Stark R, Vaitl D. 2005. Acquisition of typical EEG waveforms during fMRI: SSVEP, LRP, and frontal theta. NeuroImage. 24:1012–1024.

Senn V, Wolff SBE, Herry C, Grenier F, Ehrlich I, Gründemann J, Fadok JP, Müller C, Letzkus JJ, Lüthi A. 2014. Long-range connectivity defines behavioral specificity of amygdala neurons. Neuron. 81:428–437.

Sierra-Mercado D, Padilla-Coreano N, Quirk GJ. 2011. Dissociable roles of prelimbic and infralimbic cortices, ventral hippocampus, and basolateral amygdala in the expression and extinction of conditioned fear. Neuropsychopharmacology. 36:529–538.

Sperl MFJ, Panitz C, Hermann C, Mueller EM. 2016. A pragmatic comparison of noise burst and electric shock unconditioned stimuli for fear conditioning research with many trials. Psychophysiology. 53:1352–1365.

Tzourio-Mazoyer N, Landeau B, Papathanassiou D, Crivello F, Etard O, Delcroix N, Mazoyer B, Joliot M. 2002. Automated anatomical labeling of activations in SPM using a macroscopic anatomical parcellation of the MNI MRI single-subject brain. NeuroImage. 15:273–289.

Vansteenwegen D, Francken G, Vervliet B, de Clercq A, Eelen P. 2006. Resistance to extinction in evaluative conditioning. J Exp Psychol Anim Behav Process. 32:71–79.

Vertes RP. 2004. Differential projections of the infralimbic and prelimbic cortex in the rat. Synapse. 51:32–58.

Vidal-Gonzalez I, Vidal-Gonzalez B, Rauch SL, Quirk GJ. 2006. Microstimulation reveals opposing influences of prelimbic and infralimbic cortex on the expression of conditioned fear. Learn Mem. 13:728–733.

Walter B, Blecker C, Kirsch P, Sammer G, Schienle A, Stark R, Vaitl D. 2003. MARINA: an easy to use tool for the creation of masks for region of interest analyses. NeuroImage. 19: Supplement1. Available on CD-ROM.